iJRASET
International Journal For Research in Applied Science and Engineering Technology

INTERNATIONAL JOURNAL FOR RESEARCH

IN APPLIED SCIENCE & ENGINEERING TECHNOLOGY

Volume: 13 **Issue:** V **Month of publication:** May 2025

DOI: https://doi.org/10.22214/ijraset.2025.70200

www.ijraset.com

Call: 08813907089 | E-mail ID: ijraset@gmail.com

International Journal for Research in Applied Science & Engineering Technology (IJRASET)
ISSN: 2321-9653; IC Value: 45.98; SJ Impact Factor: 7.538
Volume 13 Issue V May 2025- Available at www.ijraset.com

Optimised Sleep Mode Activation in Cellular Networks: A Practical Case Study

Salahedin Rehan[1], Abderaof Elmrabet[2], Osama Hdida[3], Mohammed Elghadi[4]
Advanced Technology and Communication Research Group, Faculty of Engineering, University of Zawiya, Libya

Abstract: ***This paper explores the feasibility of applying sleep-mode strategies in a realistic RAN network, using a deployment scenario from a local MNO as a case study. By modelling spatially correlated shadowing and 3GPP-compliant path loss, we evaluate individual and combined eNB coverage under both optimized and sequential activation schemes. Results show that optimisation significantly improves coverage at low activation levels, achieving near-complete service with fewer active sites. A fitted similarity model characterizes convergence between the two approaches, introducing a deployment-specific parameter α that helps guide practical energy-saving decisions based on traffic load. The proposed method offers both performance gains and planning insights for dynamic, energy-aware RAN control.***

Keywords: Sleep mode, Energy efficiency, Cellular networks, Coverage optimisation, Base station activation

I. INTRODUCTION

Despite the rapid advancement of 5G technologies, LTE (4G) networks remain the backbone of global mobile communications. As of the end of 2024, 4G population coverage outside of mainland China is projected to surpass 85% globally, with expectations to reach over 95% by 2030. In contrast, 5G mid-band coverage outside of mainland China is anticipated to reach only 40% by the end of 2024. This disparity underscores the continued reliance on LTE infrastructure, particularly in regions where 5G deployment faces economic and logistical challenges [1].

Energy efficiency within Radio Access Networks (RANs) has become a central focus for both academia and industry due to the rising operational costs and carbon footprint associated with dense deployments. According to Ericsson's 2023 Mobility Report [2], 4G LTE continues to dominate the global landscape with over 5 billion subscriptions, significantly outpacing the uptake of 5G, especially in developing markets. This makes LTE a continued priority for practical energy-saving interventions. It is well established that RAN infrastructure—particularly base stations—accounts for approximately 60–80% of a mobile operator's total energy consumption [3-4]. Multiple industrial white papers, including those from Huawei [5], Nokia [6], and Samsung [7], highlight sleep-mode control as a powerful energy-saving mechanism when applied to underutilized eNBs during periods of low demand.

However, existing approaches to RAN sleep-mode control in both academic research and industrial implementations still face notable challenges. Many studies rely on heuristic or neighbour-based strategies, which, while straightforward to implement, lack scalability and generalization across different deployment scenarios [8-9]. For instance, base station on/off switching based on local traffic or reactive thresholds does not account for global spatial coverage implications and can lead to inconsistent performance. More recently, machine learning (ML)-driven techniques have gained popularity for dynamic eNB/gNB control, including reinforcement learning-based xApps in O-RAN platforms [10-11]. While these solutions show potential, they typically require large volumes of training data, are sensitive to topology and traffic distributions, and often necessitate retraining when the network changes. This makes them harder to deploy in real-world systems, particularly in legacy or LTE-based RANs where infrastructure modernization is limited [12]

In contrast, the approach proposed in this paper offers a mathematically tractable, closed-form optimisation strategy that leverages spatial RSRP maps under realistic shadowing models. It avoids the need for predictive modelling or online training, and thus remains broadly applicable, lightweight, and transparent—particularly suitable for existing LTE infrastructures where rapid, explainable energy-saving decisions are needed.

We compare two activation strategies: a sequential approach based on the individual coverage potential of each eNB and an optimisation-based approach that selects the best subset of k eNBs to maximize combined coverage. Both strategies are analysed under a 3GPP-compliant path loss model with spatially correlated log-normal shadowing.

A key contribution of our study is the introduction of a convergence model that quantifies the similarity between the optimized and sequential activation sets using the Jaccard index. The fitted exponential model, characterized by a parameter α\alphaα, encapsulates the rate at which both strategies converge in terms of coverage set similarity as more eNBs are activated.

This parameter serves as a practical planning tool, enabling operators to infer when full optimisation is necessary versus when a simpler activation heuristic suffices. Our findings are particularly relevant for operators in regions where LTE remains predominant and 5G deployment is gradual. For instance, Siemens emphasizes that 5G adoption is not a "big bang" transformation but must be smooth and phased to avoid disruptions. Similarly, Nokia reports that 60% of Communication Service Providers (CSPs) in the Middle East and Africa are adopting 5G to enhance digital transformation, indicating that a significant portion of networks still rely on LTE infrastructure [12-13].

Finally, while the operator whose deployment inspired this study has historically expressed reservations about implementing sleep-mode strategies, ongoing challenges such as frequent power outages and limitations in public grid availability make energy-aware mechanisms increasingly relevant. The findings of this study provide a structured basis for reconsideration, not only for this operator but also for operators in regions facing similar infrastructural constraints. The remainder of this paper is organized as follows: Section II details the system model and assumptions; Section III outlines the methodology; Section IV presents the results and discussion; and Section V concludes the paper with key findings and implications.

II. SYSTEM MODEL

This section details the mathematical and physical assumptions that underpin the proposed optimisation framework. The system model is intentionally structured to reflect a realistic deployment scenario, while remaining generalizable through closed-form modelling of key phenomena including propagation, shadowing, and spatial user association.

A. Network Layout and Propagation Modelling

We consider a two-dimensional service region $\mathcal{A} \subset \mathbb{R}^2$ of size $X \times Y$, over which a set of N eNodeBs (eNBs) is deployed. The eNB location are denoted by:

$$\mathcal{C} = \{c_1, c_2, \dots \dots, c_N\}, \quad c_i = (x_i, y_i) \tag{1}$$

User equipment (UE) locations are represented as a continuous spatial field, and their association is determined via maximum Reference Signal Received Power ($RSRP$) under the current activation configuration. The received signal strength at a UE from a given base station is governed by large-scale channel effects including path loss and shadowing. We define the received power $P_{rx,i}(x, y)$ from eNB_i at a 2D spatial location (x, y) as:

$$P_{rx,i}(x, y) = P_{Tx} + G_t + G_r - PL_i(x, y) - L_{RBG} \tag{2}$$

Where;

- P_{Tx} is the transmission power in dBm,
- G_t and G_r are the transmitter and receiver antenna gains, respectively, in dBi,
- $PL_i(x, y)$ is the path loss including shadowing in dB from eNB_i to location (x, y),
- $L_{RBG} = 10 \log_{10}(120)$ accounts for downscaling from total bandwidth to one Resource Block Group. This assumes 120 RBGs for a 20 MHz LTE carrier.

The pathloss model $PL_i(x, y)$ follows 3GPP Urban Macro (UMa) model [14]:

$$PL_i(x, y) = 128.1 + 37.6 \log_{10}(d_i) \tag{3}$$

Where $d_i = \sqrt{(x - x_i)^2 + (y - y_i)^2}$ is the Euclidean distance in meters between the UE and eNB_i, with a minimal distance $d_{min} = 1\, m$ to avoid singularity at where $d = 0$.

We incorporated large-scale shadowing as a spatially correlated Gaussian random field where $\mathcal{S}(x, y) \sim \mathcal{N}(0, \sigma_s^2)$ with a decaying exponential spatial autocorrelation [15][16]:

$$\mathbb{E}[\mathcal{S}(x_1, y_1)\mathcal{S}(x_2, y_2)] = \sigma_s^2 \cdot \exp\left(-\frac{||r_1 - r_2||}{d_{corr}}\right) \tag{4}$$

Where;

- d_{corr} is the spatial correlation distance,
- σ_s is the standard deviation of shadowing,
- r_1, r_2 are the 2D position vectors

The final effective path loss at location (x, y) from eNB_i becomes:

$$PL_i(x, y) = PL_{3GPP}(d_i) + \mathcal{S}(x, y) \tag{5}$$

Thus, the $RSRP$ map from eNB_i across the spatial grid is:

$$RSRP_i(x,y) = P_{Tx} + G_t + G_r - PL_{3GPP}(d_i) - \mathcal{S}(x,y) - 10\log_{10}(120) \quad (6)$$

This expression serves as the foundational input for all subsequent coverage analyses in this study. Specifically, it is evaluated across a discretised spatial grid for each eNB to generate RSRP heatmaps, which are then used to assess individual eNB coverage potential, quantify service quality under different thresholds, and support the selection of optimal subsets of active eNBs during low-traffic periods.

III.PROPOSED ENERGY-AWARE ACTIVATION STRATEGIES

This section formulates the problem of optimal eNB selection under energy-saving constraints, building directly on the physical-layer model developed in Section II. The aim is to activate the minimum number of eNBs necessary to maintain network-wide service and how many eNBs are minimally required to satisfy a given quality-of-service (QoS) constraint.

A. Problem Formulation

The optimisation problem is defined over a discretised service area and considers the aggregate downlink signal power received from active eNBs. We introduce two competing approaches for solving this problem: a low-complexity, priority-based activation scheme, and a combinatorial optimizer that guarantees selection of the best-performing set. Let the total service area be denoted by Ω, discretised into a grid of M spatial locations $\{x_1, x_2, \ldots x_M\}$. For any subset of active base stations $\mathcal{A} \subseteq \mathcal{N}$, define the received RSRP at location x_m as $RSRP(x_m; \mathcal{A})$, resulting from the combined signal of all eNBs in $\mathcal{A}$. We define the outage $\mathcal{O}_\tau(\mathcal{A})$ set under a QoS threshold τ as:

$$\mathcal{O}_\tau(\mathcal{A}) = \{x_m \in \boldsymbol{\Omega} \mid RSRP(x_m; \mathcal{A}) < \tau\} \quad (7)$$

The corresponding outage ratio is given by:

$$\epsilon(\mathcal{A}) = \frac{|\mathcal{O}_\tau(\mathcal{A})|}{M} \quad (8)$$

where $|\cdot|$ denotes set cardinality.

The operator's objective is to identify the smallest subset of active eNBs that ensures the outage ratio remains below a predefined threshold $\mathcal{E}$. Formally, the optimisation problem can be expressed as:

$$\min_{\mathcal{A} \subseteq \mathcal{N}} |\mathcal{A}| \quad subject\ to \quad \epsilon(\mathcal{A}) \leq \mathcal{E} \quad (9)$$

This formulation enables flexible adaptation to different coverage thresholds τ, outage tolerances $\mathcal{E}$, and propagation conditions. It serves as the foundation for evaluating activation strategies that balance energy efficiency with service quality.

B. Priority-Based Sequential Activation

To provide a practical and computationally light baseline for comparison, we implement a sequential activation strategy based on the individual coverage potential of each eNB. The core idea is to rank all eNBs according to their standalone ability to provide good spatial coverage. Hence, first individual average RSRP across the service area is measured and subsequently activate them in descending order of that ranking.

Let $\mathcal{N} = \{1, 2, \ldots, N\}$ be the full set of eNBs. For each $eNB_i \in \mathcal{N}$, we compute the average $RSRP$ over the grid when it is the only active transmitter denoted by $\bar{P}^{(i)}$:

$$\bar{P}^{(i)} = \frac{1}{|\mathcal{G}|} \sum_{(x,y) \in \mathcal{G}} P_{RSRP,i}(x,y) \quad (10)$$

Where $\mathcal{G}$ denotes the set of grid points covering the area, and $P_{RSRP,i}(x,y)$ is the received $RSRP$ from eNB_i at location (x,y) as derived in Section II. The eNBs are then sorted into a priority list π such that:

$$\bar{P}^{(\pi_1)} \geq \bar{P}^{(\pi_1)} \geq \ldots \geq \bar{P}^{(\pi_N)} \quad (11)$$

The sequential activation strategy activates the top-K eNBs from this list for any desired number K. That is, for a given K, the active set is:

$$\mathcal{A}_{\text{seq}}(K) = \{\pi_1, \pi_1, \ldots \ldots, \pi_K\} \quad (12)$$

This method requires no combinatorial search and is suitable for real-time or resource-limited implementations, as it avoids optimisation overhead. However, it does not account for overlapping coverage regions or spatial complementarity among eNBs, which may lead to suboptimal overall performance, particularly at low activation levels (small K). Our proposed optimisation strategy addresses this limitation in next subsection.

C. Optimized Activation via Exhaustive Coverage Maximization

While the sequential method offers simplicity, it cannot capture the complex spatial interplay among multiple eNBs. To address this limitation, we formulate a combinatorial optimisation problem where the objective is to select the best set of K active eNBs that maximizes aggregate coverage quality over the entire service area. Let:

- $\mathcal{N} = \{1,2,\dots,N\}$ denote the full set of deployed eNBs.
- $\mathcal{A} \subseteq \mathcal{N}$, $|\mathcal{A}| = K$ denote a candidate set of K active eNBs.
- $P_{RSRP,i}(x,y)$ be the $RSRP$ from eNB_i at location (x,y), as defined in Section II.

The aggregate RSRP at each location (x,y), under a given activation set $\mathcal{A}$ is:

$$P_{\text{agg}}(x,y;\mathcal{A}) = \max_{i\in\mathcal{A}} P_{RSRP,i}(x,y) \tag{13}$$

The goal is to maximize the average RSRP across the entire service area:

$$\mathcal{A}^*(K) = \arg\max_{\substack{\mathcal{A}\subseteq\mathcal{N}\\|\mathcal{A}|=K}} \left(\frac{1}{|\mathcal{G}|} \sum_{(x,y)\in\mathcal{G}} P_{\text{agg}}(x,y;\mathcal{A}) \right) \tag{14}$$

This formulation ensures that the selected eNBs provide the best joint coverage quality across the area, considering not only their individual strength but also how well they complement each other spatially. Unlike the priority-based activation in the previous subsection, this optimisation considers inter-eNB redundancy and coverage overlap, and thus can significantly reduce coverage holes, particularly for small values of K. Results in Section IV will quantitatively compare the optimized and sequential methods across various metrics.

D. Similarity Evaluation and Fitted α Modelling

To quantify the divergence between the optimized and sequential activation strategies, we introduce a set similarity metric based on Jaccard similarity [17]. The intuition is simple: if both methods select the same eNBs at a given K, then optimisation yields no gain over sequential activation, indicating natural convergence. Let:

- $\mathcal{A}^*(K)$ be the optimal set of K eNBs selected via exhaustive optimisation.
- $S(K)$ be the sequentially selected top-K eNBs based on individual coverage potential.

The Jaccard similarity index is defined as:

$$J(K) = \frac{|\mathcal{A}^*(K) \cap S(K)|}{|\mathcal{A}^*(K) \cup S(K)|} \tag{15}$$

Where $J(K) \in [0,1]$, with $J(K) = 1$ indicating perfect alignment between optimized and sequential sets, and lower values reflecting divergence. By computing $J(K)$ over a range of K we empirically observe the similarity between both schemes in terms of the selected set till they converge at a given point. To capture this convergence behaviour quantitatively, we fit an exponential model to the observed similarity curve:

$$J(K) = 1 - e^{-\alpha\,(K-K_0)} \tag{16}$$

Where;

- α is a fitted convergence rate parameter,
- K_0 is a small constant to ensure domain alignment.

The fitted α offers a compact descriptor of convergence dynamics in a given deployment. A higher α implies that optimized and sequential strategies converge rapidly, meaning fewer eNBs need to be optimized explicitly. In Section VI, we demonstrate how the derived α is used as an important Planning Utility.

IV. RESULTS AND DISCUSSION

A. Simulation Setup

The evaluation is carried out over a 4.5 km × 4.5 km service area, discretised into a 100×100 spatial grid to enable fine-grained coverage analysis. Thirteen eNBs are deployed at locations (x_i, y_i) chosen to abstract a realistic layout of a local mobile network operator (MNO). Due to security and confidentiality constraints, the exact coordinates and relative placements of actual sites could not be obtained. Instead, the deployment follows a Poisson-disc sampling algorithm with a minimum inter-site distance $D_{min} = 750$, emulating a typical dense urban microcell configuration.

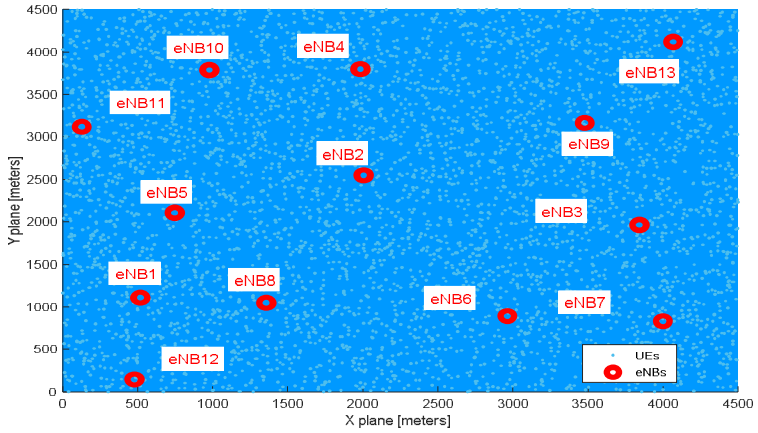

Fig. 1 Service area and placement of eNBs and UEs.

This approach ensures spatial realism while preserving generalizability. UE locations are modelled as a continuous spatial field, allowing coverage and signal strength to be evaluated across the entire service area. All evaluations incorporate the spatially correlated shadowing model, and the 3GPP-compliant path loss formulation as described in Section III. A summary of the key simulation parameters is provided in Table 1. The resulting topology is illustrated in Fig. 1.

TABLE I
SIMULATION PARAMETERS [14-16, 18-19]

Parameter	**Value / Description**
Number of eNBs	13
Minimum inter-site distance	750 [m]
Carrier frequency	2600 [Mhz]
Spectrum bandwidth	20 [Mhz]
Noise floor	-114 [dBm/Mhz]
eNB Antenna gain after cable loss	15 [dBi]
eNB noise figure	5 [dB]
Propagation model	$128.1 + 37.6 \log_{10}(d_{Km})$
lognormal shadowing std	8 dB
Shadowing Correlation Distance (d_{corr})	20 m
Antenna height	15 [m]
Transmission Power	43 [dBm]

B. Coverage Evaluation of Individual eNBs

The feasibility of eNB-level sleep modes begins with a thorough assessment of individual site coverage. Using the spatially correlated shadowing model detailed in Section III, each base station is evaluated independently. Visual coverage maps, Fig. 2 to Fig. 4, illustrate the service regions where RSRP exceeds the −130 dBm threshold, an industry-recognized lower bound for baseline service availability [19]. These regions are circled by black contour lines.

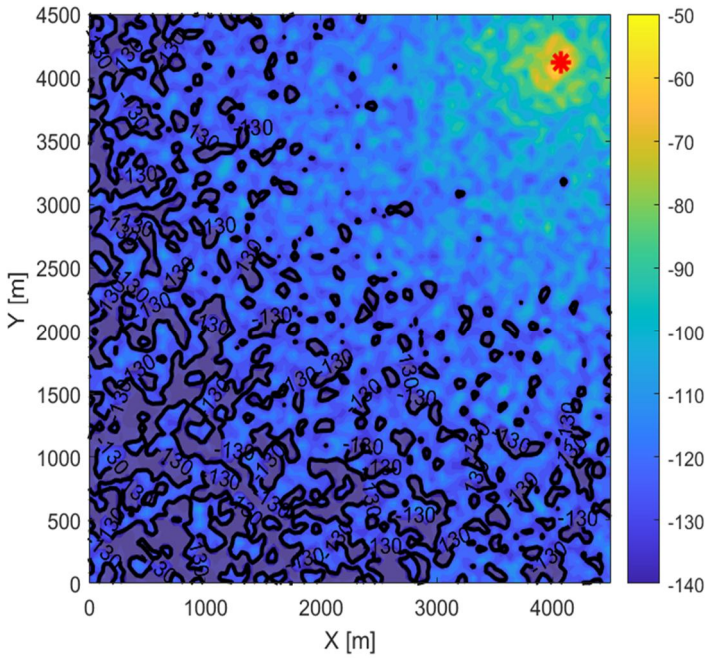

Fig. 2 eNB 13 coverage area

The findings confirm that no single eNB is capable of covering the entire region, with significant areas falling below the −130 dBm threshold in each individual map. This validates the need for multi-eNB coordination in maintaining baseline coverage hence building on the −130 dBm benchmark from, we examine how combined coverage improves when multiple eNBs are jointly activated.

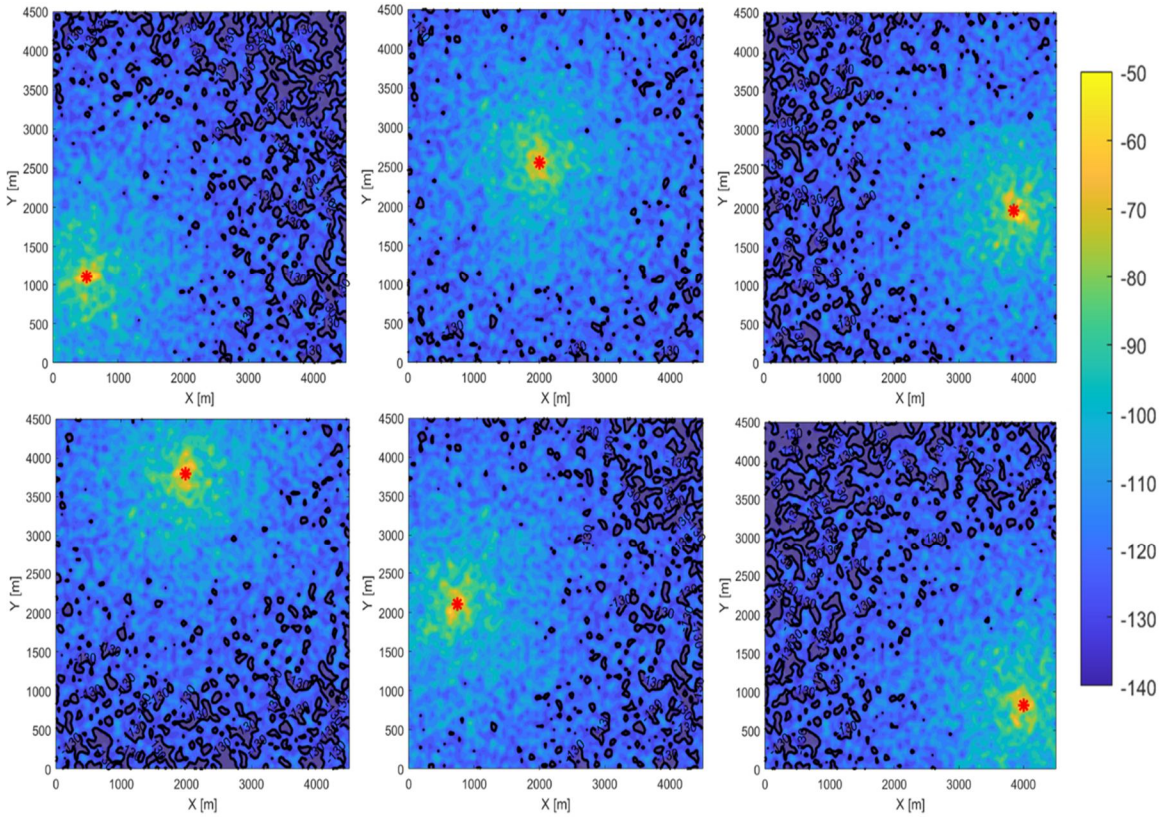

Fig. 3 eNB 1 to 6 coverage area

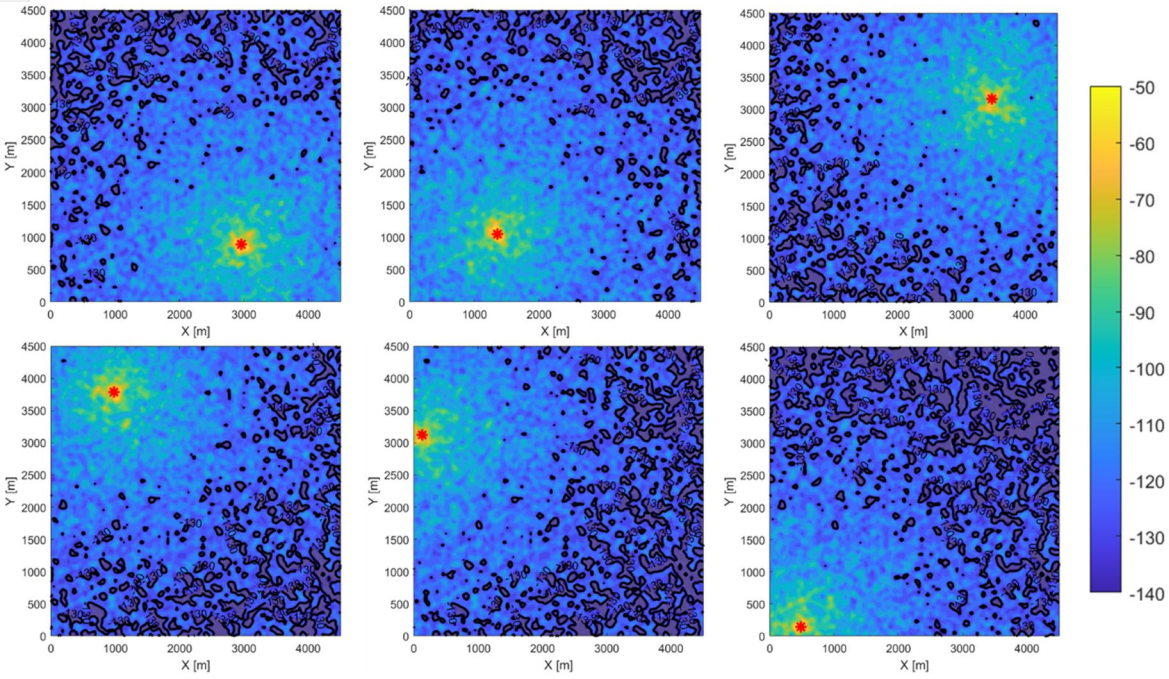

Fig. 4 eNB 7 to 12 coverage area

Fig. 5 quantifies the percentage of coverage below the -130 dBm threshold as a function of the number of active eNBs (k) under two schemes:

- Optimized activation: selecting the k-eNB subset that maximizes spatial average RSRP as per section III.
- Sequential activation: activating eNBs in ascending order of their standalone coverage strength.

The figure concludes that in order to have 99% guaranteed coverage above -130 dBm, the optimised selection scheme needs only 3 eNBs. To keep 99% guaranteed coverage, the sequential scheme based requires more than 5 eNB, doubling the number of eNBs required at very low traffic loads.

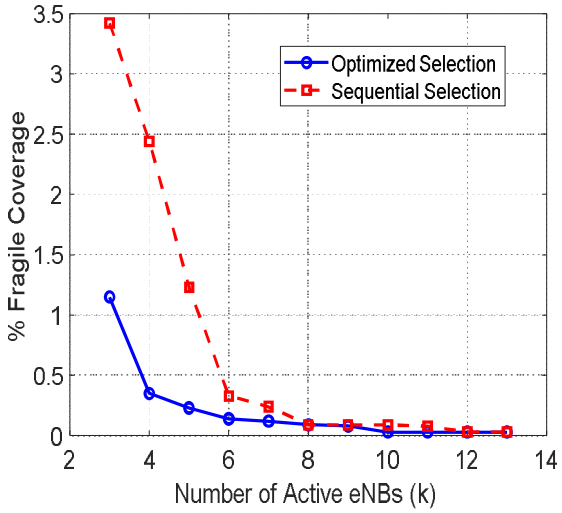

Fig. 5 percentage of coverage below -130 dBm

Fig. 6 complements this by presenting contour plots for both schemes with k = 3, visualizing the practical difference in spatial coverage. Only 1% of the area remains underserved using the optimized approach, compared to nearly 3.5% using the sequential strategy, a 3-fold improvement. This emphasizes the importance of intelligent selection in early activation stages.

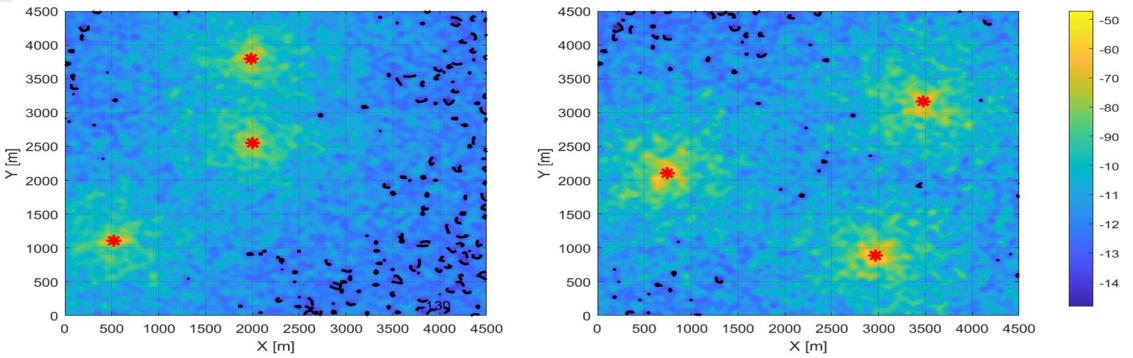

(a) Sequential selection (b) Optimised selection

Fig. 6 Coverage area at $k = 3$

Fig. 7 illustrates the percentage of the service area falling below the −140 dBm RSRP threshold, a value commonly associated with near-outage or unusable coverage conditions in 3GPP standards [19] and thus selected to represent a worst-case coverage performance boundary. At low traffic loads (i.e., fewer active eNBs), the proposed optimized selection approach demonstrates significant resilience. Specifically, it achieves 99.9% area coverage above −140 dBm with only 3 active eNBs, highlighting its robustness and suitability for deep sleep-mode scenarios. In contrast, the sequential activation scheme requires at least 5 eNBs to achieve comparable resilience, emphasizing the coverage inefficiency of non-optimized strategies during low-load periods.

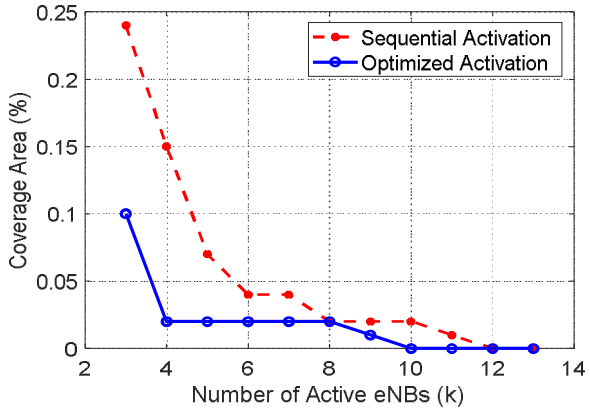

Fig. 7 Percentage of coverage area below -140 dBm

Fig. 8 shows the percentage of the area below −120 dBm, a threshold that is often used in planning guidelines to delineate the lower bound of robust or optimal LTE service quality [19]. In this context, the optimized eNB selection method maintains high-quality coverage over a greater spatial region at each activation level. With only 3 active eNBs, the optimized scheme covers over 90% of the service area above −120 dBm, while the sequential method lags behind at approximately 80% leaving a 10 percentage point coverage gap.

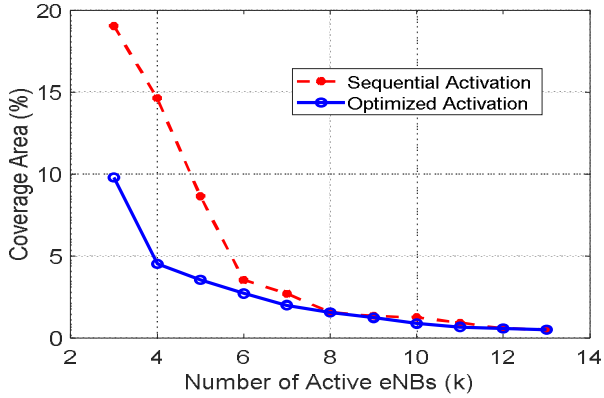

Fig. 8 Percentage of coverage below -120 dBm

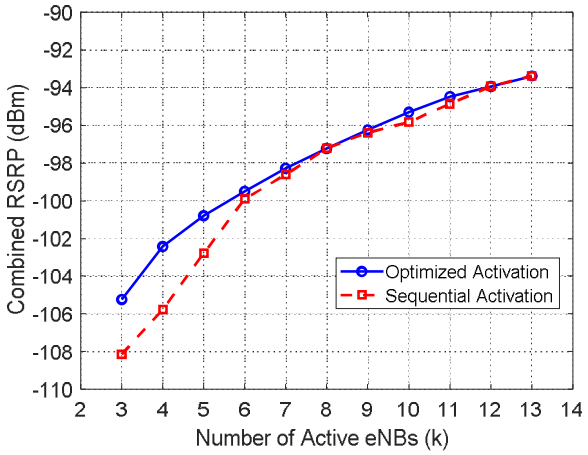

Fig. 9 Averga combined RSRP

Fig. 9 plots the average combined RSRP across all active users as k increases. As expected, the RSRP increases monotonically with the number of active eNBs due to improved spatial coverage and macro-diversity. However, the optimized activation consistently outperforms the sequential strategy in low to mid activation regimes. Regimes that are of vital importance in terms of energy efficiency. At $k = 3$, the optimized method delivers ≈3dB higher average RSRP, which translates directly to better link robustness and lower outage probability. As k increases, the performance gap gradually narrows, reflecting that the sequential approach eventually activates eNBs that are spatially diverse and contribute meaningfully to coverage. Beyond $k = 6$, both methods nearly converge, implying that optimisation has diminishing returns as full activation approaches.

In addition to mean coverage levels, Fig. 10 investigates the full distribution of RSRP values across the service area is analysed via cumulative distribution functions (CDFs), as proposed in Section 3.4. CDF curves are plotted for selected values of k $(3, 6, 9, and\ 13)$ under both the optimized and sequential selection approaches. The performance gap is most pronounced at low activation levels. At $k = 3$, the optimized method achieves almost 65% area coverage above −110 dBm, compared to only 51% with sequential selection, a relative gain of over 30%. At $k = 6$, the difference narrows but remains measurable (81.2% vs 79.7%). As k increases, the CDF curves converge, reflecting reduced benefit from optimisation at higher loads.

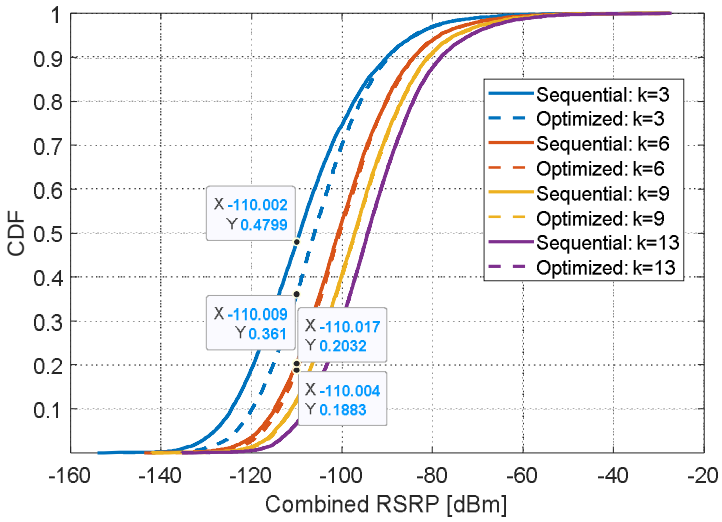

Fig. 10 Combined RSRP CDFs

To systematically quantify how the two strategies converge, we calculate the Jaccard similarity introduced in Section III-D between the sets of active eNBs chosen by each method as k increases. This is illustrated in Fig. 11. An exponential model is fitted to the empirical similarity curve, yielding a convergence parameter $\alpha = 0.2528$ fitted via nonlinear least squares. This value summarizes how quickly optimisation becomes redundant as network load increases.

Also shown is the theoretical Jaccard similarity for randomly drawn sets, which underestimates the similarity across mid-range values of k, especially between $k = 6$ and $k = 10$. This discrepancy arises because the sequential and optimized selections are not independent: both strategies prioritize high-average-RSRP nodes, thus share structural dependencies. Hence, the assumption of random independence used in the theoretical derivation does not hold in this real deployment scenario.

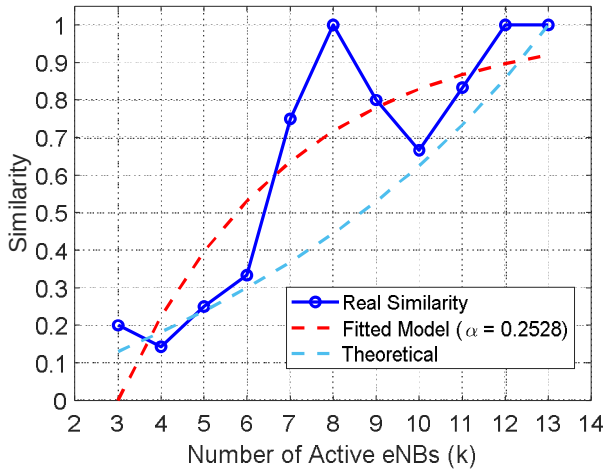

Fig. 11 Similarity and fitting vs theoretical Jaccard

As illustrated in the figure, similarity increases with k, since both methods tend to include core high-coverage eNBs as the number of active nodes grows. Thus, confirming that optimisation offers the most significant gains in low-load conditions. The high similarity observed at $k > 7$ supports the use of simplified activation during high traffic without major coverage loss. The fitted exponential model also aligns well with this trend, allowing us to extract an α value that provides actionable design insights for the studied cluster such as:

1) Planning Guidance: For $k < 7$, optimisation offers tangible gains in both coverage and quality; beyond that, simpler sequential strategies suffice.
2) Scalability Projections: The convergence model enables early estimations of required active nodes under future densification scenarios.
3) Dynamic Sleep-Mode Control: α can guide real-time algorithms. For instance, apply full optimisation under light loads, low k, and switch to sequential activation as load grows.

V. CONCLUSION

This study investigated the feasibility of eNB sleep-mode activation in a realistic LTE deployment modelled on a local operator's macro-cellular network.

Leveraging 3GPP-compliant path loss with spatially correlated shadowing and real-world inter-site spacing, we evaluated optimized versus sequential activation schemes across varying traffic conditions.

Results showed that optimized activation significantly improves coverage and efficiency in low-load scenarios. At the −140 dBm worst-case coverage threshold, 99.9% area coverage was achieved using only 3 eNBs, compared to 5 required in the sequential method. Average RSRP and CDF analyses further confirmed that optimized schemes yield stronger service quality for a given number of active eNBs, particularly when k is small.

Importantly, the derived convergence parameter α, obtained through Jaccard similarity modeling, provides a compact yet informative descriptor of how rapidly sequential and optimized strategies align as load increases. This makes α a practical planning metric, enabling operators to estimate when optimisation yields meaningful gains versus when simple sequential reactivation suffices, thereby guiding hybrid strategies that dynamically balance energy savings, performance robustness, and computational complexity. This provides a practical framework that can be directly integrated into operator planning tools for energy-aware RAN control.

REFERENCES

[1] Ericsson, "5G network coverage outlook," Ericsson Mobility Report, Nov. 2024. [Online]. Available:https://www.ericsson.com/en/reports-and-papers/mobility-report/dataforecasts/network-coverageericsson.com+1ericsson.com+1
[2] Ericsson, "Ericsson Mobility Report: November 2023," Ericsson, 2023. [Online]. Available: https://www.ericsson.com/en/reports-and-papers/mobility-report/dataforecasts/mobile-subscriptions
[3] F. Richter, A. Fehske, and G. Fettweis, "Energy Efficiency Aspects of Base Station Deployment Strategies for Cellular Networks," Proc. IEEE VTC, 2009.
[4] G. Auer et al., "How much energy is needed to run a wireless network?," IEEE Wireless Communications, vol. 18, no. 5, pp. 40–49, Oct. 2011.
[5] Huawei, "Energy Efficiency White Paper," Huawei Technologies, 2022.
[6] Nokia, "Sustainable Networks: Powering Energy Efficiency," White Paper, 2023.
[7] Samsung, "5G and Green ICT: Samsung Sustainability Report," 2023.
[8] L. M. P. Larsen et al., "Toward Greener 5G and Beyond Radio Access Networks—A Survey," IEEE Open Journal of the Communications Society, vol. 4, pp. 768–786, Mar. 2023. doi: 10.1109/OJCOMS.2023.3257889
[9] L. Kundu, X. Lin, and R. Gadiyar, "Toward Energy Efficient RAN: From Industry Standards to Trending Practice," IEEE Wireless Communications, vol. 32, no. 1, pp. 36–45, Feb. 2025.
[10] H. Alshaer et al., "Energy Saving in 6G O-RAN Using DQN-Based xApp," Proc. IEEE International Conference on Communications Workshops (ICC Workshops), 2024.
[11] A. Chatzopoulos et al., "Energy-Efficient Power Management for O-RAN Base Stations Utilizing Pedestrian Flow Analytics and Non-Terrestrial Networks," Proc. IEEE ICC, 2024.
[12] Siemens, "Private 5G & Advanced connectivity for industries," Siemens AG, 2024. [Online]. Available: https://assets.new.siemens.com/siemens/assets/api/uuid%3Aafe5e219-9669-4210-aab0-6ffb55670e3b/5-Flexible-Production-for-Industry-5G.pdfPress Release Distribution Services+2Siemens Assets+2Siemens Assets+2
[13] Nokia, "Nokia MEA Mobile Broadband Index 2024: 5G driving rapid digital transformation," Nokia Corporation, Oct. 2024. [Online]. Available: https://www.nokia.com/about-us/news/releases/2024/10/15/nokia-mea-mobile-broadband-index-2024-5g-driving-rapid-digital-transformation/Nokia.com
[14] 3GPP TR 36.814 V9.0.0, “Further advancements for E-UTRA physical layer aspects (Release 9),” Mar. 2010.
[15] 3GPP TR 36.873 V12.2.0, “Study on 3D channel model for LTE,” Jun. 2015.
[16] T. S. Rappaport, R. W. Heath, R. C. Daniels, and J. N. Murdock, Millimeter Wave Wireless Communications, Pearson Education, 2015.
[17] M. S. Islam, M. M. Billah, M. M. Rahman and S. M. Ahsan, “Performance evaluation of different similarity indices for link prediction in social networks,” in Proc. IEEE International Conference on Informatics, Electronics & Vision (ICIEV), Dhaka, Bangladesh, 2013, pp. 1–6. doi: 10.1109/ICIEV.2013.6572655
[18] 3GPP TR 38.901 V16.1.0, “Study on channel model for frequencies from 0.5 to 100 GHz (Release 16),”.
[19] 3GPP TS 36.133 V15.3.0, “Evolved Universal Terrestrial Radio Access (E-UTRA); Requirements for support of radio resource management,”.

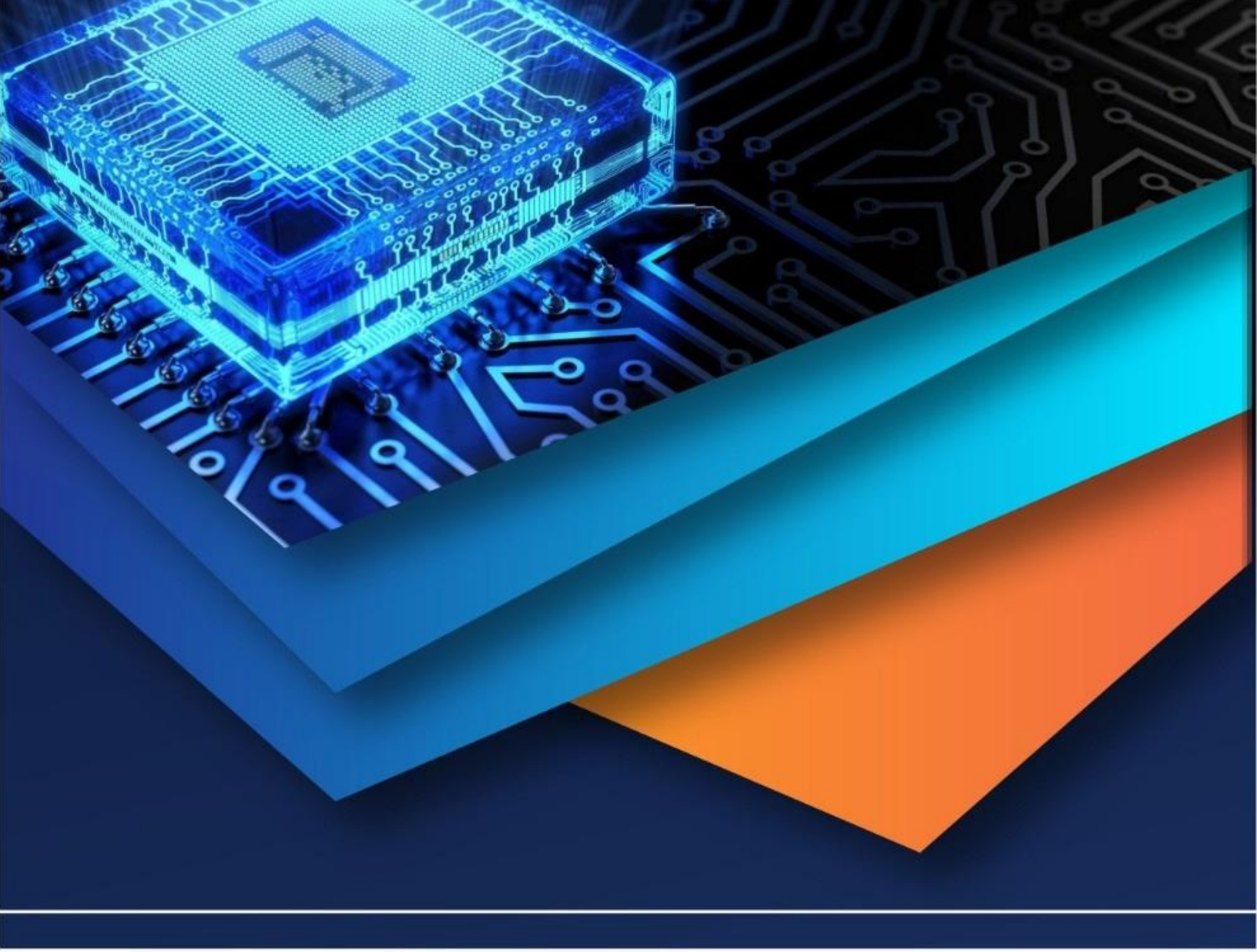

10.22214/IJRASET

45.98

IMPACT FACTOR: 7.129

IMPACT FACTOR: 7.429

INTERNATIONAL JOURNAL FOR RESEARCH

IN APPLIED SCIENCE & ENGINEERING TECHNOLOGY